NANO LETTERS

pubs.acs.org/NanoLett

Single-Molecule Kinetics and Super-Resolution Microscopy by Fluorescence Imaging of Transient Binding on DNA Origami

Ralf Jungmann,[†,§,#] Christian Steinhauer,[‡,§,#] Max Scheible,[†] Anton Kuzyk,[†] Philip Tinnefeld*[,‡,§,∥] and Friedrich C. Simmel*[,†,§]

[†]Lehrstuhl für Bioelektronik, Physik-Department, Technische Universität München, James-Franck-Strasse 1, 85748 Garching, Germany, [‡]Angewandte Physik—Biophysik, Ludwig-Maximilians-Universität, Amalienstrasse 54, 80799 München, Germany, [§]Center for NanoScience, Ludwig-Maximilians-Universität, Schellingstrasse 4, 80799 München, Germany, and [∥]Physikalische und Theoretische Chemie - NanoBioScience, Technische Universität Braunschweig, Hans-Sommer-Strasse 10, 38106 Braunschweig, Germany

ABSTRACT DNA origami is a powerful method for the programmable assembly of nanoscale molecular structures. For applications of these structures as functional biomaterials, the study of reaction kinetics and dynamic processes in real time and with high spatial resolution becomes increasingly important. We present a single-molecule assay for the study of binding and unbinding kinetics on DNA origami. We find that the kinetics of hybridization to single-stranded extensions on DNA origami is similar to isolated substrate-immobilized DNA with a slight position dependence on the origami. On the basis of the knowledge of the kinetics, we exploit reversible specific binding of labeled oligonucleotides to DNA nanostructures for PAINT (points accumulation for imaging in nanoscale topography) imaging with <30 nm resolution. The method is demonstrated for flat monomeric DNA structures as well as multimeric, ribbon-like DNA structures.

KEYWORDS Nanobiotechnology, biophysics, DNA origami, fluorescence microscopy, super-resolution, single-molecule kinetics

Recently, the field of DNA nanotechnology[1,2] has been revolutionized by the invention of the DNA origami technique,[3] which has enabled molecular engineers to build two- and even three-dimensional[4,5] structures of almost any arbitrary shape. For applications as functional materials—as the basis of synthetic biological systems or as platform for artificial molecular machines—dynamic processes on these nanoscale scaffolds become increasingly important. The DNA origami technique is based on the sequence-specific binding of hundreds of short synthetic DNA "staple" strands to a long single-stranded DNA scaffold molecule, e.g., the 7249 nt long single strand DNA genome of phage M13mp18.[3] Hybridization between the staples and the scaffold strand folds the scaffold into a two- or three-dimensional structure whose shape can be specified by the choice of the staple strand sequences. The resulting structures can be "addressed"—i.e., functionalized—with nanometer precision. Since DNA origami structures allow the organization of small molecules, proteins, aptamers, or nanoparticles into specified geometries,[6−8] they represent promising scaffolds for molecular computation, artificial molecular machines, molecular assembly lines, nanorobots, and factories.[9,10] Such applications imply dynamic processes and require dynamic functional imaging in real time with high spatial resolution. An excellent tool to monitor such processes is single-molecule fluorescence. However, it has rarely been employed in the field of DNA nanotechnology.

Here we introduce a single-molecule assay for dynamic binding and dissociation of short fluorescently labeled DNA oligonucleotides to single-stranded docking strands protruding, e.g., from DNA nanostructures. We used this assay to determine kinetic rates and varied parameters such as length of the docking strands, concentrations, temperature, and binding site location on the nanostructure, thus obtaining design rules for simple dynamic processes on DNA nanostructures.

We then used the resulting, controllable ON/OFF-switching of fluorescence by binding and dissociation for super-resolution (SR) imaging of DNA nanostructures based on subsequent localizations of single molecules. Recently, the importance of dark states for far-field SR microscopy has been realized (see, e.g., ref 11). Dark states can be obtained photophysically using photochromic compounds[12−14] or intrinsic dark states.[15−17] An alternative approach, first described by Sharonov et al.,[18] called PAINT (points accumulation for imaging in nanoscale topography) uses continuously targeting the objects to be imaged by diffusing molecules. We implemented the PAINT concept by means of reversible labeling with diffusing DNA probes. This implementation will be called DNA-PAINT throughout this Letter. In comparison to conventional labeling of nanostructures,[19,20]

* To whom correspondence should be addressed, (F.C.S.) simmel@ph.tum.de or (P.T.) philip.tinnefeld@physik.uni-muenchen.de.

[#] These authors contributed equally to this work.

Received for review: 09/29/2010
Published on Web: 00/00/0000

DOI: 10.1021/nl103427w | *Nano Lett.* **XXXX,** *xxx,* 000–000

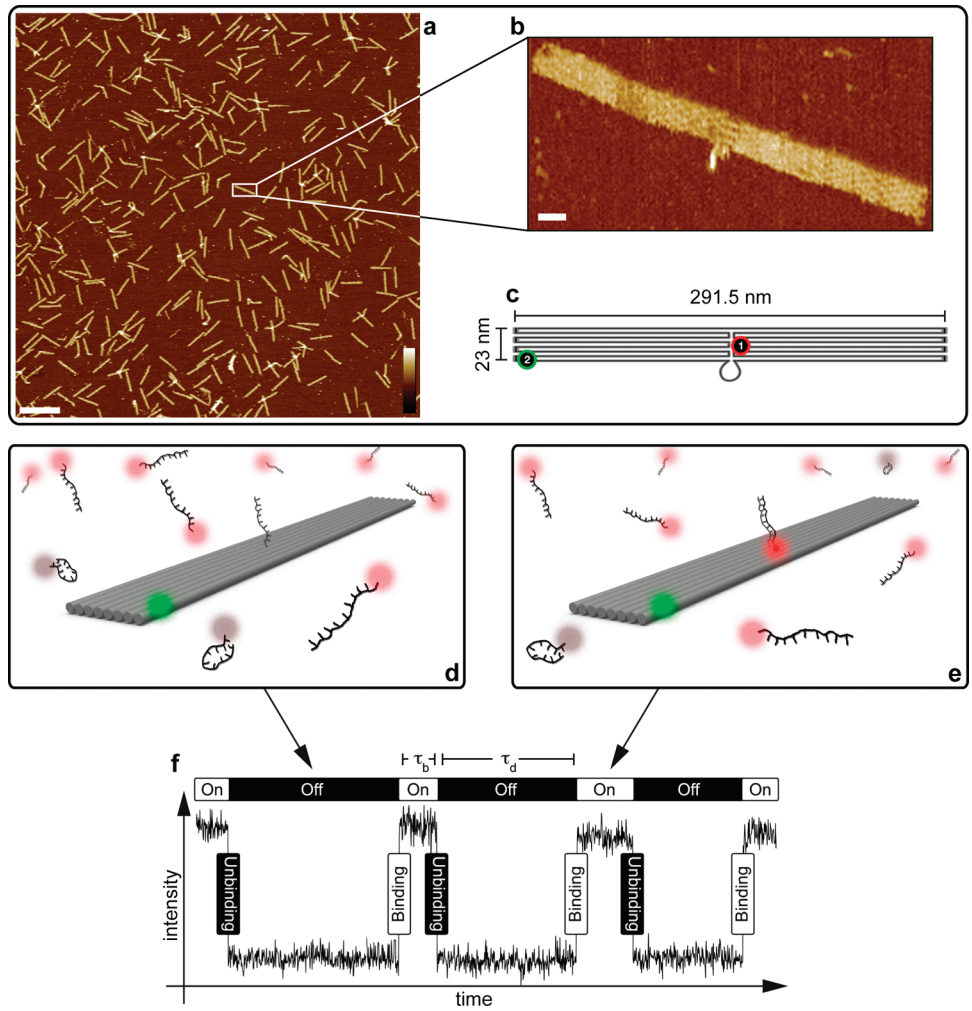

FIGURE 1. (a−c) Long rectangular DNA origami structures (LR origami, nominally 291.5 × 23 nm) are designed for the single-molecule binding/dissociation assay. (a) The solution AFM image (length scale, 500 nm; *z*-scale, 6 nm) shows a high yield of correctly formed structures (cf. Figure S1a in the Supporting Information) (b) Zoom-in on one of the LROs reveals features of the underlying double crossover substructure such as the bridged seam in the middle (length scale, 20 nm). (c) Each LRO carries a fluorescently labeled staple strand (labeled with ATTO532, represented by the green framed "2"), which is incorporated directly into the folded structure, as well as a single-stranded extension (docking strand) of a different staple strand (highlighted by the red bordered "1"). The docking strand length can, in principle, be chosen arbitrarily; in this study, the length is varied between 7 and 10 bases. Along with these modifications, five staple strands (not shown in the scheme) were labeled with biotin, protruding to the opposite side of the fluorophore and single-stranded extension strands.[19] (d−f) After formation and purification of the LROs, structures were immobilized via the biotinylated strands to a BSA/biotin/streptavidin coated coverslip and subsequently transferred to an inverted fluorescence microscope operated in TIR-Mode. Using a 650 nm laser, transient binding events of the imager strand to the LROs are monitored. (d) Scheme showing a DNA origami structure with attached ATTO532 dye (green) and red ATTO655 imager strands in solution. The docking strand extension is shown at the center of the structure. Without binding of the imager strand, no fluorescence in TIR-Mode is observed. This resembles the fluorescent OFF-state. (e) Upon hybridization of an imager strand to the docking strand on the LRO, a bright fluorescence in the red channel is observed. In TIRFM an evanescent wave excites fluorophores close to a surface, thus minimizing background fluorescence from molecules in solution (i.e., unbound). In addition, a 70% increase in fluorescence upon binding is achieved compared to the unbound state (dim fluorescence of entangled imager strands in solution, cf. Figure S3 in the Supporting Information).[21] (f) A typical intensity vs time trace is shown with low fluorescence for the unbound or dissociated state (τ_d is the time for the dissociated state) and high fluorescence upon binding of the imager strand (τ_b is the time for the bound state).

DNA-PAINT is not subject to photobleaching (the imager strands are dynamically replenished), it is free in the choice of fluorophores, and it is not prone to labeling errors or inactive fluorophores. Furthermore, DNA-PAINT has the advantage of full control over probe hybridization/dissociation kinetics.

We fabricated long rectangular 2D origami (LRO) structures with dimensions of ≈290 × 23 nm (Figure 1c) that turned out to fold correctly with high yield (cf. Figure 1a,b and Figure S1a in the Supporting Information). As indicated in Figure 1c−e, each origami structure was equipped with a fluorescently labeled staple strand (green) and one or more docking strands (red in Figure 1c).

After formation and purification, LROs were immobilized to a coverslip and imaged with a fluorescence microscope operated in total internal reflection (TIR, for experimental details see Supporting Information and ref 19). First, a "conventional" diffraction-limited image using the directly

DOI: 10.1021/nl103427w | *Nano Lett.* **XXXX,** *xxx,* 000−000

incorporated fluorescent label (here ATTO532 using an excitation wavelength of 532 nm) is acquired to determine the positions of the origami structures on the surface. In a second step, ATTO655 labeled imager strands—having a complementary sequence to the docking strands on the LROs—are added to the solution. The lengths of the imager strands are selected to result only in short-term binding events at ambient conditions. A second excitation wavelength (650 nm for ATTO655) is used to monitor the transient binding of single imager strands to the LROs.

A representative fluorescence intensity trace is shown in Figure 1f: a low signal corresponds to an unoccupied staple strand, binding of an imager strand results in a fluorescence increase. The perfect superposition of the green marker image (ATTO532) with a standard deviation image that highlights the imager strand (ATTO655) locations—based on the maximum signal variation—indicates the high selectivity of binding to DNA origami (cf. Figure S2 in the Supporting Information). Due to TIR excitation, the technique is relatively uncompromised by the fluorescent background caused by freely diffusing imager strands. Additionally, intrastrand guanine quenching is considerably reduced upon hybridization, resulting in a fluorescence increase of 70% upon binding[21] (cf. Figure 1d,e and Figure S3 in the Supporting Information).

Single-Molecule Binding Kinetics. By monitoring individual hybridization events on origami in real time as shown in Figure 1f, the association rate k_{on} can be calculated from the mean interevent lifetime ("dark" or "dissociated" time τ_d) via $1/\tau_d = k_{on}c$, where c is the imager strand concentration. From a plot of $1/\tau_d$ vs c (Figure 2a), the association rate is determined to be $k_{on} = 2.3 \times 10^6\ M^{-1}\ s^{-1}$ (for 600 mM NaCl, comparable to ensemble measurements[22−24]).

The fact that we detected the same fluorescence periods at different excitation intensities ensured that the measured binding time ("bright" or "bound" time τ_b) is not compromised by photobleaching. Hence, we could directly determine the dissociation rate $k_{off} = 1/\tau_b$ of the imager strands. As expected for a first-order reaction, k_{off} is independent of c. However, k_{off} is strongly dependent on the length of the duplex formed by imager and docking strands ($k_{off} = 1.6\ s^{-1}$ for 9 bp and $k_{off} = 0.2\ s^{-1}$ for 10 bp), while k_{on} is only weakly dependent on this length (cf. Figure 2b). Theoretically, the dissociation rate is exponentially dependent on the duplex length (see Supporting Information), and this fact can be used to adjust τ_b. Furthermore, k_{on} is slightly decreasing, while k_{off} is increasing with temperature (Figure 2c).

Positional Dependence of Binding Kinetics on DNA Origami. To check for the effect of the DNA nanostructure on the binding kinetics and to investigate positional effects as reported recently,[6] we hybridized imager strands to docking strands located at the center or edge of origami structures. We performed this study with the LROs, as well as with the more common ≈100 × 70 nm origami rectangle[3] (regular rectangle origami, "RRO", cf. Figure S4 in the Supporting Information). Kinetic rate constants for the LROs were very similar to those obtained for a control strand immobilized to the surface via a biotin−streptavidin linkage and did not show any significant position dependence. For the RROs, k_{on} was slightly reduced compared to the control. Furthermore, the center position of the RRO showed a 30% increase of k_{off} compared to the edge positions (see Table S5 in the Supporting Information for all data). Our results show a weaker position dependence than previous studies that investigated hybridization to origami structures in free solution.[6] This indicates that the conformational state of DNA origami—which is different in free solution as compared to rigidly immobilized[19]—is likely to have a stronger influence on hybridization kinetics than, e.g., locally varying electric fields.

Super-Resolution Imaging of DNA Origami Structures. Origami structures are commonly imaged using atomic force microscopy (AFM) or electron microscopy with a typical resolution in the nanometer and even subnanometer regime. However, these methods lack, so far, the ability of nondestructive monitoring of biologically relevant dynamic processes and the determination of kinetics in the subsecond range which can easily be accessed by fluorescence spectroscopy. Although high-speed AFM can compete in imaging speeds,[25] it is still limited to a small observation area and is more invasive compared to fluorescence microscopy methods. While the implementation of spectroscopic approaches with high temporal resolution should be straightforward, it is more difficult to record data with high spatial resolution and over long periods of time due to the diffraction limit and photobleaching. The common principle of imaging beyond the diffraction limit by subsequent single-molecule localizations is that only one fluorophore is active for a diffraction-limited area at any given time. This fluorophore is localized by imaging with a sensitive camera and the molecules' positions are histogramed to obtain the reconstructed super-resolved images.

As test structures for SR microscopy, we manufactured micrometer-long DNA ribbons by multimerization of LRO monomers that contained DNA-PAINT docking strands every 21.6 nm (cf. Figure 3a). As revealed by AFM imaging, multimerization results in elongated ribbons and circularized structures (cf. Figure 3a,I and Figure S7 in the Supporting Information). It is impossible to resolve the circularized structures by conventional diffraction-limited light microscopy (cf. Figure 3a,III). However, circular structures can be well resolved with DNA-PAINT using 7 nt long docking sequences (Figure 3a,II).

We also produced point patterns based on oligomerized LROs containing docking strands at distances of 32 nm at end-to-end contacts and 129.5 nm between two points within a single origami monomer (Figure 3b). As imager strands, we used Cy3b-labeled oligonucleotides to show that imaging is not restricted to ATTO655. Furthermore, this shorter wavelength dye creates a smaller point spread

DOI: 10.1021/nl103427w | *Nano Lett.* **XXXX,** *xxx,* 000–000

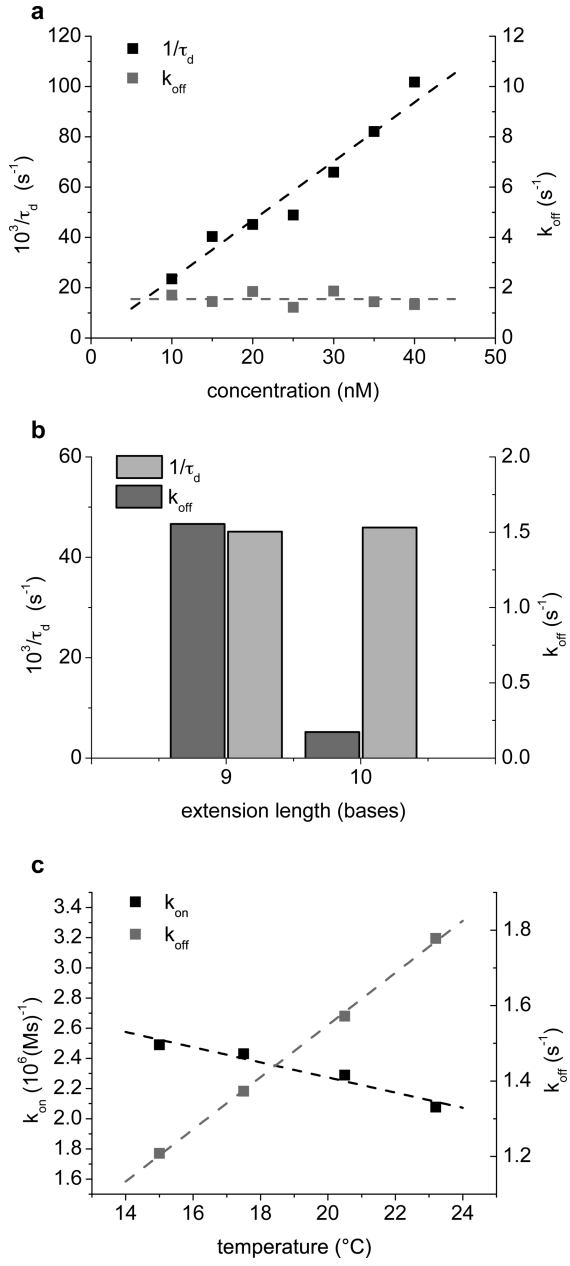

FIGURE 2. (a−c) DNA-PAINT uses fluorescently labeled single-stranded DNA probes in solution that hybridize to complementary single-stranded extension on DNA origami structures, thus imaging them in real time. Single-molecule DNA binding and unbinding events are directly visualized using fluorescence microscopy, making DNA-PAINT, apart from its imaging capabilities, an ideal tool for analyzing, e.g., hybridization kinetics on DNA structures. The strand dissociation rate (k_{off}) can directly be derived from the binding event lifetime (τ_b) from $k_{off} = 1/\tau_b$ and the association rate (k_{on}) can be calculated by a linear fit to $1/\tau_d = k_{on}c$ given the interevent lifetime (τ_d) at different imager strand concentrations (c). (a) The reciprocal of the interevent lifetime τ_d exhibits a linear dependence on the concentration of the imager strand. The linear fit yields an association rate k_{on} of 2.3×10^6 M^{-1} s^{-1} at a salt concentration of 600 mM NaCl. The dissociation rate k_{off} is independent of the imager strand concentration, as expected for a first-order reaction. (b) k_{off} is highly dependent on the length of the extension strand on the surface ($k_{off} = 1.6$ s^{-1} for the 9-mer and $k_{off} = 0.2$ s^{-1} for the 10-mer), while τ_d and thus k_{on} is only weakly dependent on the strand length. (c) Temperature dependence of hybridization rates.

function (PSF) and therefore improves the localization precision, and hence resolution.[26] With a localization accuracy of 20 ± 7 nm (mean ± fwhm), the long distances can be very well resolved (cf. Figure 3b) and the small distances are also resolved in some cases (cf. Figure S6 in the Supporting Information).

In order to precisely measure the distance between docking sites, we also imaged LRO monomers using DNA-PAINT. Figure 3c shows images and a distance distribution histogram for the monomers. The fitted distance of 111 ± 27 nm of adjacent points and 212 ± 44 nm between the outer points is slightly lower than expected from the design. This discrepancy can be accounted for by the bending of LROs that are attached to the surface via biotin linkers[19] (cf. Figure S1b in the Supporting Information).

To demonstrate the tunability of DNA-PAINT, we used different imager strands for the different imaging requirements in Figure 3. For the LRO oligomers with the highest labeling density (Figure 3a), we chose a 7 nt long docking sequence for short τ_b (<60 ms). We here used a camera frame rate of 50 Hz for image acquisition, which minimized drift effects. In contrast, for "ruler" applications[19] as in Figure 3b,c, we used a smaller label density of three dye molecules per PSF. This reduces the probability of having several emitters within a PSF at the same time. For precise distance measurements, longer binding events are desired. We therefore chose a 9 bp imager/docking duplex and a slightly lower camera frame rate of 30 Hz.

Many additional parameters are available to adjust the reaction kinetics, e.g., temperature, salt concentration, crowding agents, unlabeled competitor strands, and of course DNA sequence and secondary structure. The versatility of this sequence-programmable DNA-based imaging technique could be easily extended to multiplexed imaging by using several differently labeled imager sequences.

Imaging Efficiency. The precise control over number and position of docking strands on monomeric DNA origami structures makes it possible to quantify a quasi-labeling efficiency for DNA-PAINT imaging. We addressed the question what fraction of docking strand positions present could actually be imaged. This is an open issue for all super-resolution approaches, since many labeling positions might not actually be labeled; a fraction of fluorophores bleaches during photoactivation steps or the number of emitted photons before photobleaching is not sufficient for precise localization. For PALM, for example, only due to the latter criterion, >30% of the labeled molecules are not included in the analysis.[12]

To investigate the imaging efficiency, we carried out a comparison between the presence of staple strands at specified positions using AFM and DNA-PAINT measurements. We first studied the incorporation yield of three biotinylated staple strands into the RROs (originally used for glass surface immobilization).[19] To highlight the biotinylated strands, streptavidin was added to the origami sample on a

DOI: 10.1021/nl103427w | Nano Lett. XXXX, xxx, 000–000

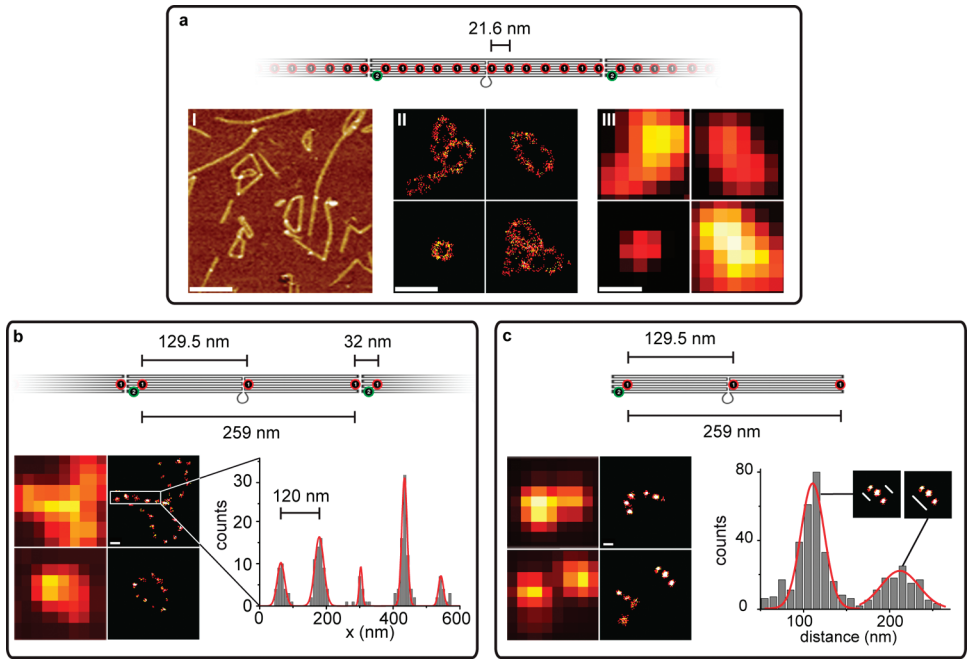

FIGURE 3. Using the precise control over fluorescent ON and OFF times of the imaging strands, localization based SR microscopy of DNA origami structures can be directly achieved using DNA-PAINT without changes to the setup or imaging conditions. (a) LRO oligomers with DNA attachment points every 21.6 nm imaged with AFM (I), DNA-PAINT (II), and diffraction-limited standard deviation imaging (III), scale bars are 500 nm. (II) and (III) show the same structures super-resolved and diffraction-limited, respectively. (b) Diffraction-limited TIRF and super-resolved DNA-PAINT images of triple labeled oligomers with connection strands every 129.5 and 32 nm. 1D histogram of a region of interest containing several attachment sites (length scale, 120 nm). (c) Distance distribution histogram of triple labeled LRO monomers (length scale, 120 nm).

mica surface and incubated for several hours. Different concentrations of streptavidin yielded identical results, indicating that binding to biotin was saturated. In AFM images we counted the number of structures carrying three or two streptavidin highlighted staple strands (for details see the Supporting Information and Figure S7). Only structures carrying three or two streptavidin molecules were counted, because only these structures could unambiguously be distinguished in fluorescence measurements using DNA-PAINT (fluorescence emission from a single point could still be due to unspecific binding or impurities).

The AFM study showed that 61 % of the structures carried three streptavidin proteins and 39 % carried two ($n = 392$). With DNA-PAINT of structures, such as depicted in Figure 3c, we were able to resolve three points in 58 % and two points in 42 % of the cases ($n = 73$). This shows the extraordinary high overall imaging efficiency of ≈95 %, clearly exceeding that of other super-resolution approaches. In addition, this is a useful feature for testing the presence of individual staple strands in functionalized origami nanoarrays. While one end of the staple can be labeled with the modification of interest, the other end carries the PAINT sequence for imaging just those positions of interest.

Discussion. We have introduced a single-molecule assay to study dynamic processes on DNA nanostructures using fluorescence microscopy. The assay allows to routinely perform analysis of DNA binding and dissociation kinetics on the single-molecule level.

As one application of the method, we investigated the position dependence of binding kinetics on several DNA origami substrates. We found a slight spatial heterogeneity of the kinetics on the origami structures that was consistent with values previously obtained in solution. We further developed the assay to a super-resolution microscopy technique (DNA-PAINT) that exploits the transient binding of fluorescently labeled DNA imager strands to DNA docking strands and is thus ideally suited for the characterization of DNA-based nanostructures such as DNA origami. In contrast to previously published PAINT approaches[18,27] our method offers the advantages of sequence specificity (hence multiplexing capabilities) and wide adjustability of ON and OFF times. Another advantage of DNA-PAINT is that it is not limited by photobleaching and that almost all docking strands are imaged (efficiency ≈95 %). The temporal resolution is somewhat limited by the concentration of fluorophores in solution; however imaging of processes on the time scale of minutes (as, e.g., in ref 9) is possible with DNA-PAINT. Improved self-quenching of the probe in its unbound state will further accelerate the measurements. With appropriate labeling protocol this method could be extended to imaging biological samples by conjugation of DNA to an antibody.

DNA-PAINT is a comparatively simple technique and can easily be implemented on any sensitive wide-field fluorescence microscope without further modifications. Acquired data can be readily analyzed and visualized using a freely

DOI: 10.1021/nl103427w | *Nano Lett.* **XXXX,** *xxx,* 000–000

available data analysis and visualization software package programmed in LabVIEW. The software—together with sample data sets from this paper and online documentation—can be downloaded for free at http://www.e14.ph.tum.de. Future applications of single-molecule fluorescence in DNA nanotechnology are envisioned in the analysis of spatiotemporal reaction cascades and biosensors[6,28,29] based on DNA origami and the study of DNA-based molecular motors and machines.[9,10,30]

Acknowledgment. This work was supported by the DFG (Inst 86/1051-1 and through the Excellence Cluster Nanosystems Initiative Munich), the Biophotonics Program of the BMBF/VDI, the LMU Center for Nanoscience, and the Elitenetzwerk Bayern. The authors thank Helene Budjarek for experimental support and Hendrik Dietz, Carsten Forthmann, Tim Liedl, and Stephan Renner for helpful discussions.

Supporting Information Available. Detailed description of materials and methods and additional figures and tables. This material is available free of charge via the Internet at http://pubs.acs.org.

REFERENCES AND NOTES

(1) LaBean, T. H.; Li, H. Constructing novel materials with DNA. *Nano Today* **2007**, *2*, 26–35.
(2) Zhang, C.; He, Y.; Su, M.; Ko, S. H.; Ye, T.; Leng, Y.; Sun, X.; Ribbe, A. E.; Jiangh, W.; Mao, C. DNA self-assembly: from 2D to 3D. *Faraday Discuss.* **2009**, *143*, 221–233.
(3) Rothemund, P. W. K. Folding DNA to create nanoscale shapes and patterns. *Nature* **2006**, *440*, 297–302.
(4) Andersen, E. S.; Dong, M.; Nielsen, M. M.; Jahn, K.; Subramani, R.; Mamdouh, W.; Golas, M. M.; Sander, B.; Stark, H.; Oliveira, C. L. P.; Pedersen, J. S.; Birkedal, V.; Besenbacher, F.; Gothelf, K. V.; Kjems, J. Self-assembly of a nanoscale DNA box with a controllable lid. *Nature* **2009**, *459*, 73–75.
(5) Douglas, S. M.; Dietz, H.; Liedl, T.; Högberg, B.; Graf, F.; Shih, W. M. Self-assembly of DNA into nanoscale three-dimensional shapes. *Nature* **2009**, *459*, 414–418.
(6) Ke, Y. G.; Lindsay, S.; Chang, Y.; Liu, Y.; Yan, H. Self-assembled water-soluble nucleic acid probe tiles for label-free RNA hybridization assays. *Science* **2008**, *319*, 180–183.
(7) Maune, H. T.; Han, S.-P.; Barish, R. D.; Bockrath, M.; Iii, W. A. G.; Rothemund, P. W. K.; Winfree, E. Self-assembly of carbon nanotubes into two-dimensional geometries using DNA origami templates. *Nat. Nanotechnol.* **2009**, *5*, 61–66.
(8) Hung, A. M.; Micheel, C. M.; Bozano, L. D.; Osterbur, L. W.; Wallraff, G. M.; Cha, J. N. Large-area spatially ordered arrays of gold nanoparticles directed by lithographically confined DNA origami. *Nat. Nanotechnol.* **2010**, *5*, 121–126.
(9) Lund, K.; Manzo, A. J.; Dabby, N.; Michelotti, N.; Johnson-Buck, A.; Nangreave, J.; Taylor, S.; Pei, R.; Stojanovic, M. N.; Walter, N. G.; Winfree, E.; Yan, H. Molecular robots guided by prescriptive landscapes. *Nature* **2010**, *465*, 206–210.
(10) Gu, H.; Chao, J.; Xiao, S.-J.; Seeman, N. C. A proximity-based programmable DNA nanoscale assembly line. *Nature* **2010**, *465*, 202–205.
(11) Vogelsang, J.; Steinhauer, C.; Forthmann, C.; Stein, I. H.; Person-Skegro, B.; Cordes, T.; Tinnefeld, P. Make them blink: probes for super-resolution microscopy. *ChemPhysChem* **2010**, *11*, 2475–2490.
(12) Betzig, E.; Patterson, G. H.; Sougrat, R.; Lindwasser, O. W.; Olenych, S.; Bonifacino, J. S.; Davidson, M. W.; Lippincott-Schwartz, J.; Hess, H. F. Imaging intracellular fluorescent proteins at nanometer resolution. *Science* **2006**, *313*, 1642–1645.
(13) Rust, M. J.; Bates, M.; Zhuang, X. Sub-diffraction-limit imaging by stochastic optical reconstruction microscopy (STORM). *Nat. Methods* **2006**, *3*, 793–795.
(14) Hess, S. T.; Girirajan, T. P.; Mason, M. D. Ultra-high resolution imaging by fluorescence photoactivation localization microscopy. *Biophys. J.* **2006**, *91*, 4258–4272.
(15) Folling, J.; Bossi, M.; Bock, H.; Medda, R.; Wurm, C. A.; Hein, B.; Jakobs, S.; Eggeling, C.; Hell, S. W. Fluorescence nanoscopy by ground-state depletion and single-molecule return. *Nat. Methods* **2008**, *5*, 943–945.
(16) Steinhauer, C.; Forthmann, C.; Vogelsang, J.; Tinnefeld, P. Superresolution microscopy on the basis of engineered dark states. *J. Am. Chem. Soc.* **2008**, *130*, 16840–16841.
(17) van de Linde, S.; Kasper, R.; Heilemann, M.; Sauer, M. Photoswitching microscopy with standard fluorophores. *Appl. Phys. B: Lasers Opt.* **2008**, *93*, 725–731.
(18) Sharonov, A.; Hochstrasser, R. M. Wide-field subdiffraction imaging by accumulated binding of diffusing probes. *Proc. Natl. Acad. Sci. U.S.A.* **2006**, *103*, 18911–18916.
(19) Steinhauer, C.; Jungmann, R.; Sobey, T.; Simmel, F.; Tinnefeld, P. DNA origami as a nanoscopic ruler for super-resolution microscopy. *Angew. Chem., Int. Ed.* **2009**, *48*, 8870–8873.
(20) Flors, C.; Ravarani, C. N.; Dryden, D. T. Super-resolution imaging of DNA labelled with intercalating dyes. *ChemPhysChem* **2009**, *10*, 2201–2204.
(21) Doose, S.; Neuweiler, H.; Sauer, M. Fluorescence quenching by photoinduced electron transfer: a reporter for conformational dynamics of macromolecules. *ChemPhysChem* **2009**, *10*, 1389–1398.
(22) Henry, M. R.; Stevens, P. W.; Sun, J.; Kelso, D. M. Real-time measurements of DNA hybridization on microparticles with fluorescence resonance energy transfer. *Anal. Biochem.* **1999**, *276*, 204–214.
(23) Lehr, H. P.; Reimann, M.; Brandenburg, A.; Sulz, G.; Klapproth, H. Real-time detection of nucleic acid interactions by total internal reflection fluorescence. *Anal. Chem.* **2003**, *75*, 2414–2420.
(24) Michel, W.; Mai, T.; Naiser, T.; Ott, A. Optical study of DNA surface hybridization reveals DNA surface density as a key parameter for microarray hybridization kinetics. *Biophys. J.* **2007**, *92*, 999–1004.
(25) Endo, M.; Katsuda, Y.; Hidaka, K.; Sugiyama, H. Regulation of DNA methylation using different tensions of double strands constructed in a defined DNA nanostructure. *J. Am. Chem. Soc.* **2010**, *132*, 1592–1597.
(26) Bobroff, N. Position measurement with a resolution and noise-limited instrument. *Rev. Sci. Instrum.* **1986**, *57*, 1152–1157.
(27) Giannone, G.; Hosy, E.; Levet, F.; Constals, A.; Schulze, K.; Sobolevsky, A. I.; Rosconi, M. P.; Gouaux, E.; Tampe, R.; Choquet, D.; Cognet, L. Dynamic superresolution imaging of endogenous proteins on living cells at ultra-high density. *Biophys. J.* **2010**, *99*, 1303–1310.
(28) Wilner, O. I.; Weizmann, Y.; Gill, R.; Lioubashevski, O.; Freeman, R.; Willner, I. Enzyme cascades activated on topologically programmed DNA scaffolds. *Nat. Nanotechnol.* **2009**, *4*, 249–254.
(29) Voigt, N. V.; Torring, T.; Rotaru, A.; Jacobsen, M. F.; Ravnsbaek, J. B.; Subramani, R.; Mamdouh, W.; Kjems, J.; Mokhir, A.; Besenbacher, F.; Gothelf, K. V. Single-molecule chemical reactions on DNA origami. *Nat. Nanotechnol.* **2010**, *5*, 200–203.
(30) Green, S. J.; Bath, J.; Turberfield, A. J. Coordinated chemomechanical cycles: a mechanism for autonomous molecular motion. *Phys. Rev. Lett.* **2008**, *101*, 238101.

DOI: 10.1021/nl103427w | *Nano Lett.* **XXXX,** *xxx,* 000–000